Journal of Sound and Vibration (2000) **229**(4), 993–1002
doi:10.1006/jsvi.1999.2507, available online at http://www.idealibrary.com on IDEAL®

LETTERS TO THE EDITOR

TORSIONAL INSTABILITIES AND NON-LINEAR OSCILLATION OF A SYSTEM INCORPORATING A HOOKE'S JOINT

S. I. CHANG

Department of Environmental Engineering, University of Seoul, 90 Jeonnong-dong, Dongdaemun-gu, Seoul 130-743, *Korea*

(*Received* 6 *March* 1998, *and in final form* 28 *June* 1999)

1. INTRODUCTION

Hooke's joint is a commonly used element in drive trains to transmit twisting moment from an input shaft to an output shaft. The kinematic relation between the input and output angles induces periodically varying velocity ratios and it is known that this can cause violent torsional oscillations of the torsionally flexible shafts within certain ranges of rotating speed.

For the prediction of such critical speed ranges a one-degree-of-freedom model was considered by Porter [1]. The non-linear governing equation was derived and linearized to the equation with time-varying coefficients. Floquet theory [2] was applied to the equation to obtain the stability map. It was shown that when the ratio of the natural frequency of the straightened system (i.e., the system when Hooke's joint angle is zero) to the input rotating speed is integral or nearly integral, such critical speed ranges exist. He also found that Hooke's joint angle and the ratio of the input and output shafts determine the widths of these speed ranges.

Porter and Gregory [3] applied the classical method of Kryloff and Bogoliuboff [4] to the original non-linear equation of motion for the prediction of the amplitude of the oscillations. A set of the equations for the amplitude and phase of limit cycle was obtained in terms of Bessel functions of the first kind. It was shown that multiple limit cycles may exist at a specific input rotating speed and that an appropriate shock may induce a shift from one limit cycle to the other limit cycle which may have larger amplitude of the oscillation.

In the present work, the non-linear equation of motion in Porter [1] is revisited. Based on Floquet theory, the higher order stability map for the damped system is obtained by using a perturbation technique. By proper rescalings and transformations of the variables and parameters, the equation of motion in the so-called standard form [5] is obtained. The application of higher order averaging [6] to this equation of motion produces the amplitude equations in truncated form. The amplitude equations consist of a finite number of terms including quadratic and cubic non-linearities. The steady state response diagrams produced by the amplitude equations show that multiple stable solutions co-exist and that jump

0022-460X/00/040993 + 10 $35.00/0

phenomena [2] can occur. The amplitude equations are used to determine the basins of attraction of the stable solutions.

2. EQUATION OF MOTION

As shown in Figure 1, the system under investigation consists of a rigid body of moment of inertia, I, which is driven through a Hooke's joint and two torsionally flexible shafts. The shafts are uniform along the length and the constant torsional stiffnesses of the input and output shafts are s_1 and s_2 respectively. The input angular velocity, Ω, is kept constant. The input and output angles of the joint are α and β respectively. It is assumed that the source of energy loss of the system is the viscous damping, c, exerted on the rotating body, I. The angle of rotation of the rigid body, I, is θ. The angular misalignment, λ of the two shafts, is assumed to be small. No lateral vibration is possible with ideal long bearings.

The dimensionless equation of motion for the relative torsional displacement, i.e., the twist of the input shaft, is given in Porter and Gregory [3] as follows:

$$\begin{aligned}
&\ddot{x} + K^2 x + 2vK(\dot{x} + \rho) \\
&\quad + \varepsilon[\{(\rho - \tfrac{3}{2})\cos(2x + 2\tau) - \tfrac{3}{2}\}\ddot{x} \\
&\quad - \rho(\dot{x} + 1)^2 \sin(2x + 2\tau) \\
&\quad + \{(1 - \rho)\ddot{x}\sin(2x + 2\tau) + 2(1 - \rho)(\dot{x} + 1)^2 \cos(2x + 2\tau) \\
&\quad - \tfrac{3}{2}K^2(1 + \cos(2x + 2\tau))\}x \\
&\quad + 2(1 - \rho)\dot{x}(\dot{x} + 1)\sin(2x + 2\tau)] = 0,
\end{aligned} \tag{1}$$

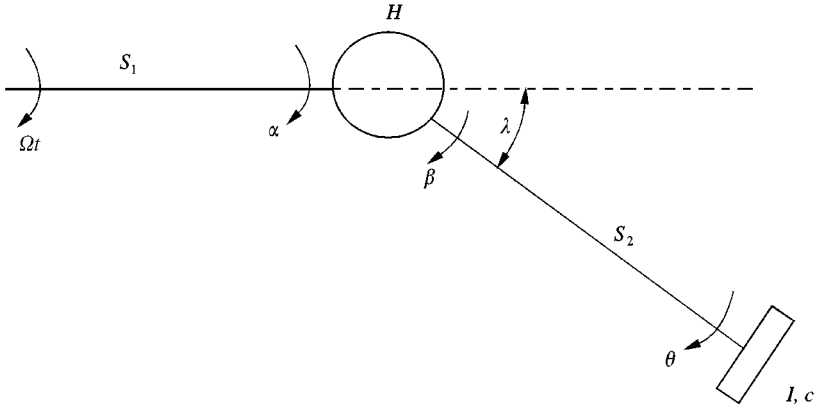

Figure 1. Diagram of the system.

where the dot represents differentiation with respect to τ, which is equal to Ωt. The x is the relative torsional displacement of the input shaft, $\alpha - \tau$. The K is defined as the ratio of linear natural frequency $\omega = \sqrt{s_1 s_2 / I(s_1 + s_2)}$, and input angular velocity, Ω. The ρ is the ratio of the output shaft stiffness, s_2, and the stiffness of the whole linear system, $s_1 + s_2$. The ε has been set to $\sin^2 \lambda$, and v is $c/2\omega I$.

Expanding equation (1) about $x = 0$ in Taylor series and performing appropriate algebra can convert the equation into the form $\ddot{x} + f(x, \dot{x}, t) = 0$ as follows:

$$\begin{aligned}
&\ddot{x} + K^2 x + 2vK(\dot{x} + \rho) \\
&\quad + \varepsilon[\, -\rho \sin(2\tau) - 4x\rho \cos(2\tau) + 2\dot{x} \sin(2\tau) \\
&\quad + 2\dot{x}^2 \sin(2\tau) + 6\rho x^2 \sin(2\tau) \\
&\quad - 2x^3 K^2 \cos(2\tau) - 8\rho x \dot{x}^2 \cos(2\tau) + \cdots\,] = 0. \qquad (2)
\end{aligned}$$

As shown in equation (2), the system has the linear and non-linear parametric and external excitations. The excitations are inherent due to the Hooke's joint and the misalignment of the two shafts. As shown in equation (2), parametric resonances can occur for the cases, $K \approx 1, 2, 3, 4, \ldots$, [7]. Among them, the cases, $K \approx 1$ and $K \approx 2$ which correspond to the principal and secondary parametric resonances, respectively, are considered. When $K \approx 1$, the principal parametric resonance will play an important role in determining the response of the system, but when $K \approx 2$, the resonance due to the external excitation as well as the secondary parametric resonance will give significant contribution to the response of the system. It is noted that ε and ρ play the roles of the amplitudes of the various external and parametric excitations.

3. ANALYSIS

Based on Floquet theory, the method of strained parameters [2] is used to obtain the transition curves in the stability map. Then the method of averaging is applied to get amplitude equations of motion, from which steady state constant solutions are obtained. The procedures for higher order averaging can be found in reference [6], which this analysis follows closely.

3.1. PARAMETRIC INSTABILITIES

The problem of dynamic stability of parametrically excited system has been studied extensively [2, 7]. The stability map in parameter space can be constructed by utilizing Floquet theory. As noted in the previous section, the present system has the parametric and external excitations simultaneously. In order to study the dynamic instability due to the parametric resonance, the original equation of motion, equations (1) or (2), is linearized to the form $\ddot{x} + f(t)x + g(t)\dot{x} = F(t)$ and the corresponding homogeneous system $\ddot{x} + f(t)x + g(t)\dot{x} = 0$ is used for the study of the parametric instabilities. The method of strained parameters [2] is used to obtain explicit expressions for the transition curves of the stability map.

When $K \approx 1$, the variables and parameters in equation (2) are rescaled as

$$x = \varepsilon z, \qquad v = \varepsilon \mu. \tag{3}$$

Then equation (2) is converted to

$$\ddot{z} + K^2 z + 2\mu K \rho - \rho \sin(2\tau) + O(\varepsilon) = 0. \tag{4}$$

Applying a transformation

$$z = y + \frac{\rho}{K^2 - 2^2} \sin 2\tau - \frac{2\mu\rho}{K}, \tag{5}$$

where y is assumed to have the period, 2π, to the linearized form of equation (4) gives

$$\ddot{y} + f_1(\tau, K, \rho, \mu, \varepsilon) y + g_1(\tau, K, \rho, \mu, \varepsilon)\dot{y} = F_1(\tau, K, \rho, \mu, \varepsilon), \tag{6}$$

where $f_1(\cdot)$, $g_1(\cdot)$ and $F_1(\cdot)$ are functions of τ, K, ρ, μ and ε and their lengthy expressions are not given here. Now the method of strained parameters is applied to equation (6) with $F_1(\tau, K, \rho, \mu, \varepsilon) = 0$ to give the transition curve as follows:

$$\begin{aligned} K^2 = {} & 1^2 \pm \tfrac{1}{2}\varepsilon(\rho^2 - 16\mu^2)^{1/2} \\ & + \varepsilon^2 \{\tfrac{1}{32}(7\rho^2 + 56\rho - 32 - 64\mu^2) \pm \tfrac{3}{4}(\rho^2 - 16\mu^2)^{1/2}\} \\ & + O(\varepsilon^3). \end{aligned} \tag{7}$$

From equation (7), it is easily seen that K^2 in equation (7) is real only if $\rho^2 - 16\mu^2 \geqslant 0$. Since we assume positive damping, in terms of the original parameters it implies $v \leqslant \frac{1}{4}\varepsilon\rho$ for the parametric instability.

When $K \approx 2$, the variables and parameters in equation (2) are rescaled as

$$x = \varepsilon z, \qquad v = \varepsilon^2 \mu. \tag{8}$$

Then equation (2) becomes

$$\ddot{z} + f_2(\tau, K, \rho, \mu, \varepsilon) z + g_2(\tau, K, \rho, \mu, \varepsilon)\dot{z} = F_2(\tau, K, \rho, \mu, \varepsilon), \tag{9}$$

where $f_2(\cdot)$, $g_2(\cdot)$ and $F_2(\cdot)$ are functions of τ, K, ρ, μ and ε and their lengthy expressions are not given here. Again the method of strained parameters is applied to equation (9) with $F_2(\tau, K, \rho, \mu, \varepsilon) = 0$ to give the transition curve as follows:

$$\begin{aligned} K^2 = {} & 2^2 \\ & + \varepsilon^2 [\tfrac{1}{6}(\rho^2 + 18\rho - 6) \pm \tfrac{1}{4}\{(3\rho^2 - 6\rho - 2)^2 - 1024\mu^2\}^{1/2}] \\ & + O(\varepsilon^3). \end{aligned} \tag{10}$$

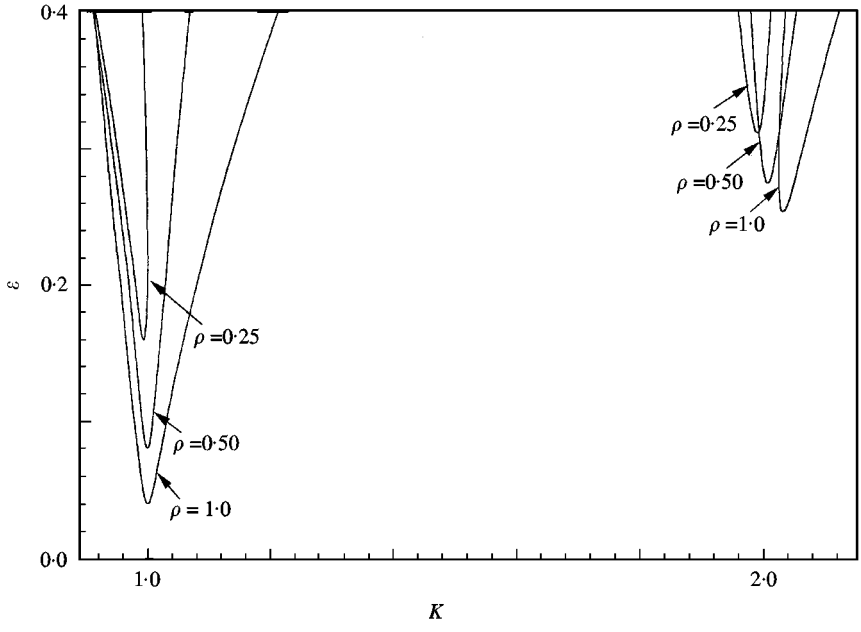

Figure 2. Stability map for $v = 0{\cdot}01$ and $\rho = 0{\cdot}25$, $0{\cdot}50$ and $1{\cdot}0$.

Similarly as for $K \approx 1$, from equation (10), it is easily seen that K^2 in equation (10) is real only if the argument inside the square root symbol is positive. Since we assume positive damping, in terms of the original parameters it implies $v \leqslant \frac{1}{32}\varepsilon^2(3\rho^2 - 6\rho - 2)$ for the parametric instability. The stability map obtained from equations (7) and (10) are shown in Figure 2, where the curves are plotted for $v = 0{\cdot}01$ and the various values of ρ. As shown in Figure 2, increasing the value of ρ has a destabilizing effect on the torsional motion of the input shaft.

3.2. HIGHER ORDER AVERAGING

As pointed out in the previous section, when $K \approx 1$, the response of this system is decided mainly by the primary parametric resonance. The variables and parameters in equation (2) are rescaled with the small parameter ε as in equation (3), and an external detuning parameter, σ, is introduced as follows:

$$K^2 = 1^2 + \varepsilon\sigma. \tag{11}$$

Then equation (2) becomes

$$\ddot{z} + z - \rho\sin(2\tau) + 2\mu\rho + \varepsilon\bar{F}_1(z,\tau) + \varepsilon^2\bar{F}_2(z,\tau) + \varepsilon^3\bar{F}_3(z,\tau) + O(\varepsilon^4) = 0, \tag{12}$$

where $\bar{F}_i$'s include various linear and non-linear terms.

By letting $x_1 = z$, $x_2 = \dot{z}$, we can express equation (12) in vector form as follows:

$$\dot{X} = AX + Q_e + \varepsilon \bar{f}_1 + \varepsilon^2 \bar{f}_2 + \varepsilon^3 \bar{f}_3 + O(\varepsilon^4), \tag{13}$$

where

$$X = \begin{pmatrix} x_1 \\ x_2 \end{pmatrix}, \qquad A = \begin{bmatrix} 0 & 1 \\ -1 & 0 \end{bmatrix}, \qquad Q_e = \begin{pmatrix} 0 \\ \rho \sin(2\tau) - 2\mu\rho \end{pmatrix},$$

$$\bar{f}_1 = \begin{pmatrix} 0 \\ -\bar{F}_1 \end{pmatrix}, \qquad \bar{f}_2 = \begin{pmatrix} 0 \\ -\bar{F}_2 \end{pmatrix} \quad \text{and} \quad \bar{f}_3 = \begin{pmatrix} 0 \\ -\bar{F}_3 \end{pmatrix}.$$

Let

$$X = \mathrm{e}^{A\tau} Y + \bar{Q}_e, \tag{14}$$

where

$$\bar{Q}_e = \begin{pmatrix} -\frac{1}{3}\rho \sin(2\tau) - 2\mu\rho \\ -\frac{2}{3}\rho \cos(2\tau) \end{pmatrix},$$

and

$$Y = \begin{pmatrix} y_1 \\ y_2 \end{pmatrix}.$$

By the transformation (14), the response z has been assumed to be in the form of

$$z = y_1 \cos\tau + y_2 \sin\tau - \tfrac{1}{3}\rho \sin 2\tau - 2\mu\rho, \tag{15}$$

which implies that the input shaft oscillates around the static twist $-2\mu\rho$. It is noted that the amount of the static twist is increased by increasing damping or the value of ρ.

Transforming equation (13) via equation (14) gives the equation in the standard form as follows:

$$\dot{Y} = \varepsilon \bar{g}_1(Y, \tau) + \varepsilon^2 \bar{g}_2(Y, \tau) + \varepsilon^3 \bar{g}_3(Y, \tau) + O(\varepsilon^4), \tag{16}$$

where $\bar{g}_i(Y, \tau) = \mathrm{e}^{-A\tau} \bar{f}_i(Y, \tau)$. By applying the method of higher order averaging [6] to equation (16), we can obtain a set of averaged equations as follows:

$$y_1' = A_1 y_1 + A_2 y_2 + A_3 y_1^2 + A_4 y_2^2 + A_5 y_1 y_2 + A_6 y_2^3 + A_7,$$

$$y_2' = B_1 y_1 + B_2 y_2 + B_3 y_1^2 + B_4 y_2^2 + B_5 y_1 y_2 + B_6 y_1^3 + B_7, \tag{17}$$

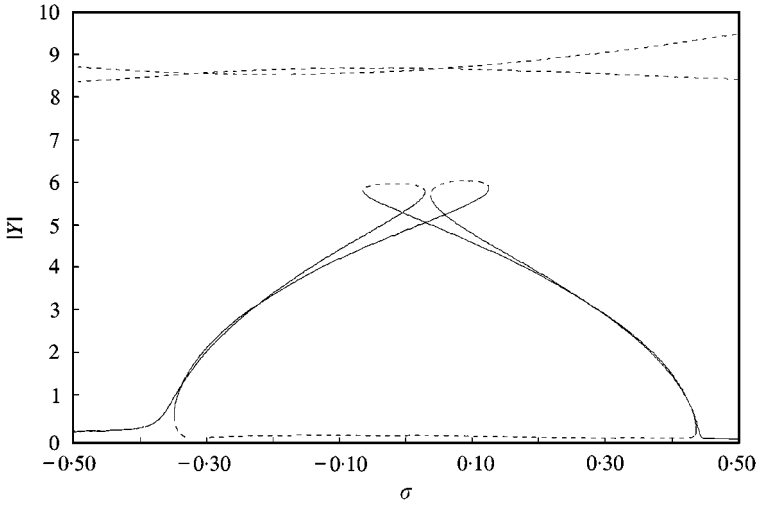

Figure 3. Response diagram ($|Y|$ versus σ) for $K \approx 1$, $\nu = 0{\cdot}01$, $\rho = 0{\cdot}6$, and $\varepsilon = 0{\cdot}19$.

where y_i''s represent the rate of change of y_i with respect to $\tilde{\tau} = \varepsilon\tau$. The coefficients A_i's and B_i's in equation (17) are the functions of the parameters, ε, μ and ρ and their lengthy expressions are not presented here. With the rescalings of equation (3), the non-linearities of the first and second order in equation (16) are diminished through the averaging process. Therefore, the non-linearities of system (1) can be captured by averaging up to the third order.

Representative response diagrams of equilibrium points of equations (17) are shown in Figure 3, where $|Y|$ is defined as $(y_1^2 + y_2^2)^{1/2}$ and the solid and broken lines represent stable and unstable solutions respectively. As shown in Figure 3, multiple stable solutions co-exist and jump phenomena can occur. The corresponding phase plot in Figure 4 shows four saddles (points a–d) and three spiral sinks (points e–g) with approximate stable and unstable manifolds. The basins of attraction for the three spiral sinks are determined by the stable manifolds of the saddle points. With the initial conditions outside the boundary consisting of the stable manifolds for the saddle points c and d, infinite responses are obtained from the averaged equations.

As noted earlier, when $K \approx 2$, the response of the system is decided by the external resonance and the secondary parametric resonance. In order to consider both effects simultaneously we rescale the variables and parameters in equation (2) as equation (8) and

$$\rho = \varepsilon\delta. \tag{18}$$

An external detuning parameter, σ, is introduced as follows:

$$K^2 = 2^2 + \varepsilon\sigma. \tag{19}$$

Then equation (2) becomes

$$\ddot{z} + 2^2 z + \varepsilon\tilde{F}_1(z, \tau) + \varepsilon^2\tilde{F}_2(z, \tau) + \varepsilon^3\tilde{F}_3(z, \tau) + O(\varepsilon^4) = 0, \tag{20}$$

where $\tilde{F}_i$'s include various linear and non-linear terms.

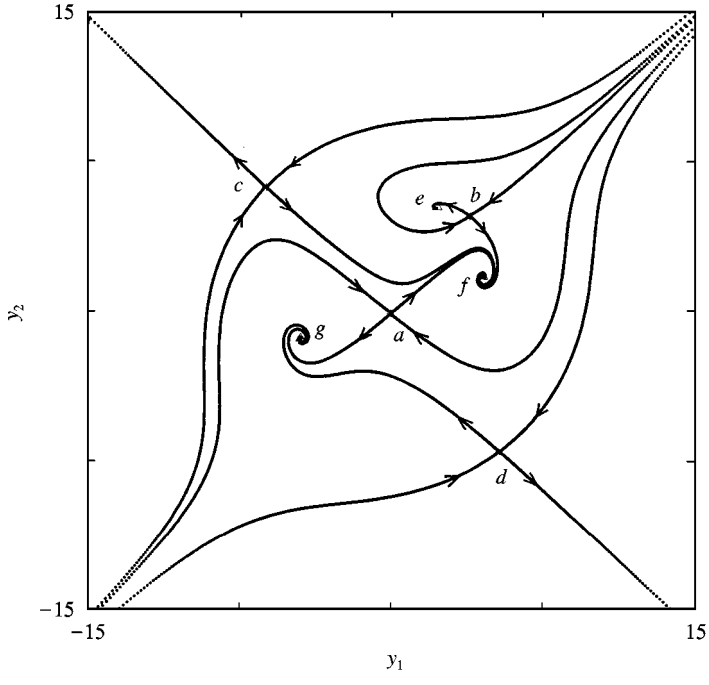

Figure 4. Phase plot for $K \approx 1$, $v = 0{\cdot}01$, $\rho = 0{\cdot}6$, $\varepsilon = 0{\cdot}19$ and $\sigma = 0{\cdot}1$.

Similarly, as for the case $K \approx 1$, by letting $x_1 = z$, $x_2 = \dot{z}$, we can express equation (20) in vector form as follows:

$$\dot{X} = \tilde{A}X + \varepsilon \tilde{f}_1 + \varepsilon^2 \tilde{f}_2 + \varepsilon^3 \tilde{f}_3 + O(\varepsilon^4), \tag{21}$$

where

$$X = \begin{pmatrix} x_1 \\ x_2 \end{pmatrix}, \qquad \tilde{A} = \begin{bmatrix} 0 & 1 \\ -2^2 & 0 \end{bmatrix},$$

$$\tilde{f}_1 = \begin{pmatrix} 0 \\ -\tilde{F}_1 \end{pmatrix}, \qquad \tilde{f}_2 = \begin{pmatrix} 0 \\ -\tilde{F}_2 \end{pmatrix} \quad \text{and} \quad \tilde{f}_3 = \begin{pmatrix} 0 \\ -\tilde{F}_3 \end{pmatrix}.$$

Let

$$X = \mathrm{e}^{\tilde{A}\tau} Y, \tag{22}$$

where

$$Y = \begin{pmatrix} y_1 \\ y_2 \end{pmatrix}.$$

By the transformation (22), the response z has been assumed to be in the form of

$$z = y_1 \cos 2\tau + y_2 \sin 2\tau, \tag{23}$$

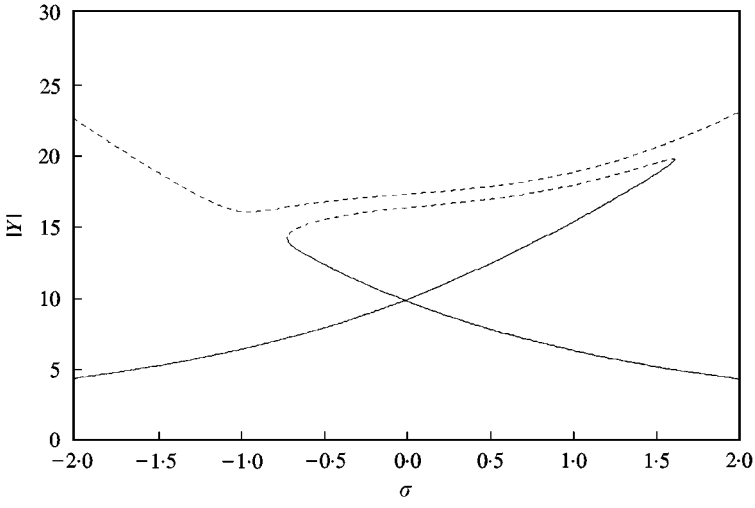

Figure 5. Response diagram ($|Y|$ versus σ) for $K \approx 2$, $\nu = 2{\cdot}0 \times 10^{-4}$, $\rho = 0{\cdot}5$, and $\varepsilon = 5{\cdot}0 \times 10^{-2}$.

where it is noted that dissimilarly as in the case of $K \approx 1$, no static twist is assumed to exist. Transforming equation (21) via equation (22) gives the equation in the standard form as follows:

$$\dot{Y} = \varepsilon \tilde{g}_1(Y, \tau) + \varepsilon^2 \tilde{g}_2(Y, \tau) + \varepsilon^3 \tilde{g}_3(Y, \tau) + O(\varepsilon^4), \tag{24}$$

where $\tilde{g}_i(Y, \tau) = \mathrm{e}^{-\tilde{A}\tau} \tilde{f}_i(Y, \tau)$. By applying the method of higher order averaging to equation (24), we can obtain a set of averaged equations as follows:

$$\begin{aligned} y_1' &= \tilde{A}_1 y_1 + \tilde{A}_2 y_2 + \tilde{A}_3 y_1^2 + \tilde{A}_4 y_2^2 + \tilde{A}_5, \\ y_2' &= \tilde{B}_1 y_1 + \tilde{B}_2 y_2 + \tilde{B}_3 y_1 y_2 + \tilde{B}_4, \end{aligned} \tag{25}$$

where the prime denotes the differentiation with respect to $\tilde{\tau} = \varepsilon\tau$. The coefficients $\tilde{A}_i$'s and $\tilde{B}_i$'s in equation (25) are also functions of the parameters, ε, μ and δ and their lengthy expressions are not presented here. It is noted that the system (25) has quadratic non-linearities only. Those can be obtained by averaging up to the third order.

Representative response diagram of equilibrium points of equations (25) are shown in Figure 5. The corresponding phase plot in Figure 6 shows two saddles (points a and b) and two sprial sinks (points c and d) with the stable and unstable manifolds. Similarly as in the case of $K \approx 1$, the basins of attraction are determined by the stable manifolds of the saddle points.

4. CONCLUSIONS

The original complex non-linear system has the inherent parametric as well as external excitations. When the rotating speed is close to the linear natural frequency, the primary parametric resonance can occur. When the rotating speed is

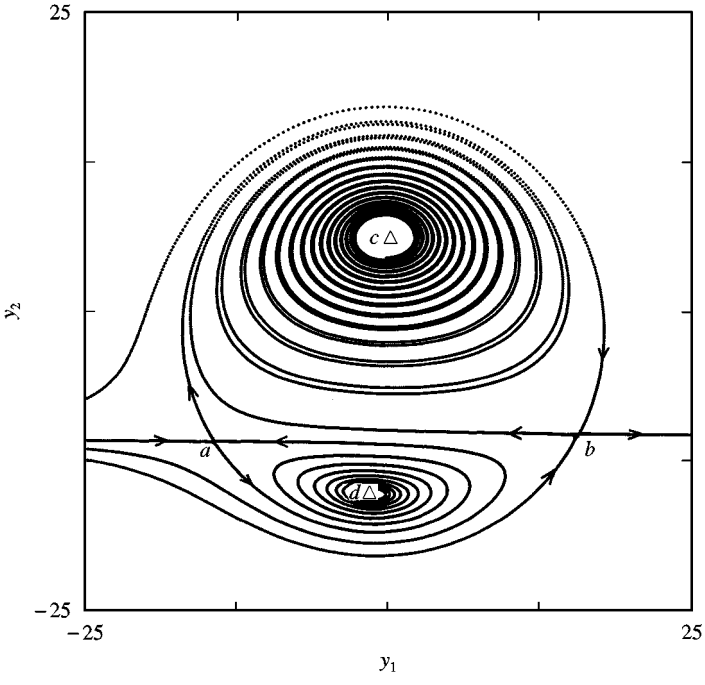

Figure 6. Phase plot for $K \approx 2$, $v = 2{\cdot}0 \times 10^{-4}$, $\rho = 0{\cdot}5$, $\varepsilon = 5{\cdot}0 \times 10^{-2}$ and $\sigma = 0{\cdot}2$.

close to half of the linear natural frequency, the external and secondary parametric resonances can occur simultaneously. By using the method of strained parameters, the higher order stability map for the damped system is obtained from the linearized model. The ratio of the stiffness of the input shaft to that of the output shaft is one of the factors that determine the parametric instability region in the map. The truncated amplitude equations of motion are obtained by applying the method of higher order averaging to the non-linear system. By plotting the averaged responses in phase plane, the basins of attraction are determined.

REFERENCES

1. B. Porter 1961 *Journal of Mechanical Engineering Science* **3**, 324–329. A theoretical analysis of the torsional oscillation of a system incorporating a Hooke's joint.
2. A. H. Nayfeh and D. T. Mook 1979 *Nonlinear Oscillations*. New York: Wiley-Interscience.
3. B. Porter and W. Gregory 1963 *Journal of Mechanical Engineering Science* **5**, 191–200. Non-linear torsional oscillation of a system incorporating a Hooke's joint.
4. N. Kryloff and N. Bogoliuboff 1947 *Annals of Mathematics Studies*, Vol. 11. Princeton: Princeton University Press. Introduction to non-linear mechanics.
5. J. Guckenheimer and P. Holmes 1983 *Applied Mathematical Sciences*, Vol. 42. New York: Springer-Verlag. Nonlinear oscillations, dynamical systems, and bifurcations of vector fields.
6. J. A. Murdock 1991 *Perturbations Theory and Methods*. New York: Wiley.
7. V. V. Bolotin 1964 *The Dynamic Stability of Elastic System*. San Francisco: Holden-day Inc.